Journal of Colloid and Interface Science 668 (2024) 142–153

Contents lists available at ScienceDirect

Journal of Colloid And Interface Science

journal homepage: www.elsevier.com/locate/jcis

Regular Article

# Developing excellent plantar pressure sensors for monitoring human motions by using highly compressible and resilient PMMA conductive iongels

Haifei Wang [a], Guanhua Lin [b,*], Yang Lin [a], Yang Cui [a], Gang Chen [b], Zhengchun Peng [a]

[a] Center for Stretchable Electronics and NanoSensors, College of Physics and Optoelectronic Engineering, Shenzhen University, Shenzhen 518060, China
[b] Strait Institute of Flexible Electronics (SIFE, Future Technologies), Fujian Key Laboratory of Flexible Electronics, Fujian Normal University and Strait Laboratory of Flexible Electronics (SLoFE), Fuzhou 350117, China

## GRAPHICAL ABSTRACT

Schematic illustration of plantar pressure distribution visualization system including a 9-channel pressure sensor array, analog to digital converter, data analysis software, and operation interface.

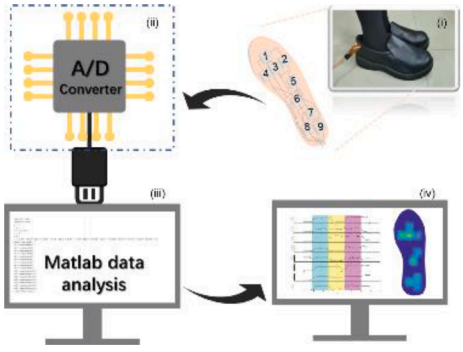


## ARTICLE INFO

*Keywords:*
Iongels
Pressure Sensor
Wearable Devices
Highly Compressible and Resilient
Human Motions

## ABSTRACT

Based on real-time detection of plantar pressure, gait recognition could provide important health information for rehabilitation administration, fatigue prevention, and sports training assessment. So far, such researches are extremely limited due to lacking of reliable, stable and comfortable plantar pressure sensors. Herein, a strategy for preparing high compression strength and resilience conductive iongels has been proposed by implanting physically entangled polymer chains with covalently cross-linked networks. The resulting iongels have excellent mechanical properties including nice compliance (young's modulus < 300 kPa), high compression strength (>10 MPa at a strain of 90 %), and good resilience (self-recovery within seconds). And capacitive pressure sensor composed by them possesses excellent sensitivity, good linear response even under very small stress (~kPa), and long-term durability (cycles > 100,000) under high-stress conditions (133 kPa). Then, capacitive pressure sensor arrays have been prepared for high-precision detection of plantar pressure spatial distribution, which also exhibit excellent sensing performances and long-term stability. Further, an extremely sensitive and fast response plantar pressure monitoring system has been designed for monitoring plantar pressure of foot at different postures

* Corresponding authors.
*E-mail addresses:* lingh@fjnu.edu.cn (G. Lin), zcpeng@szu.edu.cn (Z. Peng).

https://doi.org/10.1016/j.jcis.2024.04.137
Received 29 February 2024; Received in revised form 17 April 2024; Accepted 19 April 2024
Available online 23 April 2024

including upright, forward and backward. The system achieves real-time tracking and monitoring of changes of plantar pressure during different static and dynamic posture processes. And the characteristics of plantar pressure information can be digitally and photography displayed. Finally, we propose an intelligent framework for real-time detection of plantar pressure by combining electronic insoles with data analysis system, which presents excellent applications in sport trainings and safety precautions.

## 1. Introduction

Recently, flexible and wearable devices have attracted extensive attention due to their promising applications in human–machine interaction, smart robotics, human motion tracking, and personal healthcare monitoring [1,2]. The use of flexible and wearable devices for human motion tracking can provide important body information for further applications, such as rehabilitation administration, fatigue prevention, and sports training assessment [3–6]. Particularly, gait recognition is critical for early warning of the loss of balance events, which are the primary causes of fall injuries of construction workers, elder individuals, and patients [7,8]. Furthermore, gait recognition also can provide effective prediction of cerebellar problems caused by physiological aging, pathological aging as well as alcohol/drug-related stimulants [9]. Currently, posture monitoring has been accomplished via video-based human motion analysis technology or inertial sensor system [10]. However, the task of gait recognition remains challenging due to the complexity of collecting data on the amplitude, spatial distribution, and temporal evolution of plantar pressure. These data are mainly obtained through wearable pressure monitoring devices that need to possess the ability to detect changes in pressure information in real-time, accurately, sensitively, and reliably.

Among the wearable plantar pressure monitoring devices, flexible pressure sensors have been extensively employed to collect the plantar pressure information. The transformation of external mechanical stimuli into measurable electrical signals is based on mechanical–electrical transduction modes (e.g., piezoresistive, capacitive, piezoelectric, and triboelectric sensing mechanisms) [11–14]. In previous works, Pan and co-workers reported a smart insole system consisting of a capacitive pressure sensor array to monitor plantar pressure distributions [15]. Thanks to the introducing of a controllable vertical pore dielectric layer, their devices achieved wide detection range, high sensitivity, and real-time display of plantar pressure mapping. A pressure mapping system based on a piezoelectric nanogenerator can accurately acquire plantar pressure signals during walking [16]. The improvement of sensitivity and response speed of flexible pressure sensor could be achieved by structural design (e.g., pyramidal structures, mesh structures and micropores) [13,17,18]. However, destruction of such well-designed microstructures under persistent high-stress conditions is still a major obstacle for achieving stability and reliability of the sensing of plantar pressures. Furthermore, wearing comfort in a daily usage and prevention of foot fatigue after long-term wearing are another vital requirement. In addition, unlike flexible pressure sensors used in e-skin, artificial tactile, and bioelectronics that necessitate high sensitivity, wide response ranges, and rapid response speed, the primary challenges for plantar pressure sensors lie in ensuring reliability and stability [19–22]. For the plantar pressure sensors, they must withstand harsh working conditions, including bearing the entire body weight and enduring prolonged and repetitive trampling. As such, the production of highly flexible pressure sensors requires the use of flexible materials that possess great mechanical properties, sensing performances, long-term stability, softness and wearable comfort.

To address the mentioned concerns, conductive iongels with good mechanical flexibility and deformability are highly desired candidates for constructing wearable electronic devices [23–25]. However, there are seemingly contradictory requirements in mechanical properties when developing plantar pressure sensors, such as soft and strong, tough and resilient. These requirements hinder the application of iongels in plantar pressure sensors. So, developing new methods to fabricate iongels with excellent properties in all aspects is crucial for the synthesis of advanced wearable electronic devices. Generally, the mechanical strength is enhanced by increasing the crosslinking density in single network hydrogel to induce hydrogel hardening. In other words, the prepared hydrogels are typically more rigid. In the network hydrogel, the tough hydrogel is achieved by introducing energy dissipation unites, accompanying inevitable hysteresis in deformation, and thus tough hydrogels are typically not resilient [26–28]. Recently, a low hysteresis hydrogel has been developed by creating a polymer network with few crosslinks, where mechanical tension is transmitted along and between polymer chains, leading to enhanced mechanical properties [29]. Therefore, synthesis of physically entangled polymer chains that contains a stress transmission network will be a great approach to fabricate iongels with improved properties such as mechanical flexibility, high compressive strength, and resilience [30–32].

Herein, we reported a method for fabricating conductive iongels with high compression strength and resilience by implanting physically entangled polymer chains with covalently cross-linked secondary networks. The resulting iongels presented excellent mechanical softness (young's modulus $< 300$ kPa), high compression strength (compression stress $> 10$ MPa at a strain of 90 %), and resilience (self-recovery time within seconds). To validate their promising application as flexible pressure sensors, we prepared a capacitive pressure sensor with laminated multilayer structure by integrating iongels as flexible electrodes. As a result, the resultant capacitive pressure sensor has excellent sensing and mechanical performances, as well as good long-term stability (cycles $> 100{,}000$) during detection of pressures. Next, capacitive pressure sensor arrays have been produced for high-precision detection of plantar pressure spatial distribution. Then, a new plantar pressure monitoring system has been established for monitoring plantar pressure of feet at different postures. The system can achieve real-time tracking and monitoring of changes of plantar pressure during different static and dynamic motions. And the characteristics of plantar pressure information can be displayed digitally and photographically for further analysis and applications. Finally, we propose an intelligent framework by combining electronic insoles as capacitive pressure sensors with a data analysis system to monitor plantar pressures in real time during sports training and as a safety precaution. Hence, by forming new structures at the molecular level, this work paves the way for designing advanced materials with excellent mechanical properties, sensing performances, stability, and wearable comfort ability, and boosting their applications in the fields of wearable electronic devices and sensors. We believe that our research can play an important role in many fields such as sensing, wearable devices, robot skins, sports training, safety precautions, and medical treatments.

## 2. Experimental section

### 2.1. Chemicals

Polymethyl Methacrylate (PMMA, Sigma, Mw = 990,000 g/mol by GPC), acetone (Sinopharm Chemical Reagent Co., LTD.), 1-ethyl-3-methylimidazolium bis (trifluoromethyl sulfonyl) imide (Shanghai Cheng Jie Chemical Co., LTD), Monomer methyl methacrylate (MMA, Shanghai Aladdin Biochemical Technology), triethylene glycol dimethacrylate (TEGDMA, Aladdin), and 2-hydroxy-2-methylpropiophenone (Aladdin). All these chemicals were used as received without further

treatment. Pure water for all of the experiments was obtained from a Millipore water purification system (Millipore Corp.).

### 2.2. Preparation of iongels

The iongels were prepared by photoinitiated radical polymerization of monomer in a solution of PMMA and ionic liquid. We firstly dissolved PMMA in ionic liquid to obtain a solution via the following method: PMMA (1 g) was dissolved in acetone (9 g, analytical reagent) at room temperature under stirring for 4 h. Then, the PMMA solution (0.5 g) was added into ionic liquid (1-ethyl-3-methylimidazolium bis (trifluoromethyl sulfonyl) imide, [EMI][TFSI]) (1 g) under stirring, and the acetone was removed at 60 °C for 12 h. Secondly, we construct covalently crosslinked secondary network in the plastic iongels by polymerization of the monomer. Monomer methyl methacrylate (MMA, 0.3 g), crosslinking agent triethylene glycol dimethacrylate (TEGDMA, 10.2 mg), and photoinitiator 2-hydroxy-2-methylpropiophenone (10.0 mg) were added into the PMMA plastic iongels under vigorous agitation, then degassing under vacuum conditions for 10 min. The mixture was transferred to a transparent polymer mold (platelike (1 mm in depth) and columnar (12 mm in diameter, 25 mm in length)), and the iongels were obtained by curing the mixture under UV light (wavelength 365 nm, power 20 W) for 15 min. We prepared iongels according to the aforementioned method with various proportions of PMMA, MMA, and crosslinking agents to study the effects of polymer network on mechanical performance.

### 2.3. Construction of capacitive pressure sensors

A capacitive pressure sensor was constructed by assembling a sandwich structure with PDMS film as a dielectric layer and iongel as an electrode layer. The PDMS film was prepared by mixing the base and curing agent (Sylgard 184, Dow Corning) in a weight ratio of 10:1. The liquid mixture was degassed and thermally cured at 60 °C for 2 h. We stacked two layers of iongels films on the two surfaces of the PDMS film. The silver paint was coated on the iongels to connect with metal wires. Then the device was encapsulated by PDMS as a protective layer. The assembly of electronic insoles using a flexible printing circuit on a polyimide (PI) substrate to construct a capacitive pressure sensor.

### 2.4. Chemical characterization and measurement

Thermogravimetry analysis (TGA, Q50, TA Instruments) and differential scanning calorimetry (DSC 200 F3, NETZSCH) were measured to study thermal properties, the samples were heated from room temperature to 600 °C with heating rates 10 °C/min. The airflow rate was maintained at 20 mL/min. Optical images were collected by a digital camera. The electrical tests were carried out by the electric impedance at a voltage of 0.5 V in a frequency of 10–$10^5$ Hz. The compression tests were performed by a mechanical testing machine (Instron E1000) with a 1000 N load cell. A columnar test sample with a diameter of 12 mm and length of about 10–15 mm was compressed at a speed of 5 mm/min at room temperature. The results were collected from at least three times tests for the same sample. The resilience test was conducted by loading–unloading cycles with a compression strain of 75 % at a speed of 5 mm/min.

## 3. Results and discussions

### 3.1. Design principle of physically entangled structures

In general, optimal plantar pressure sensors with outstanding

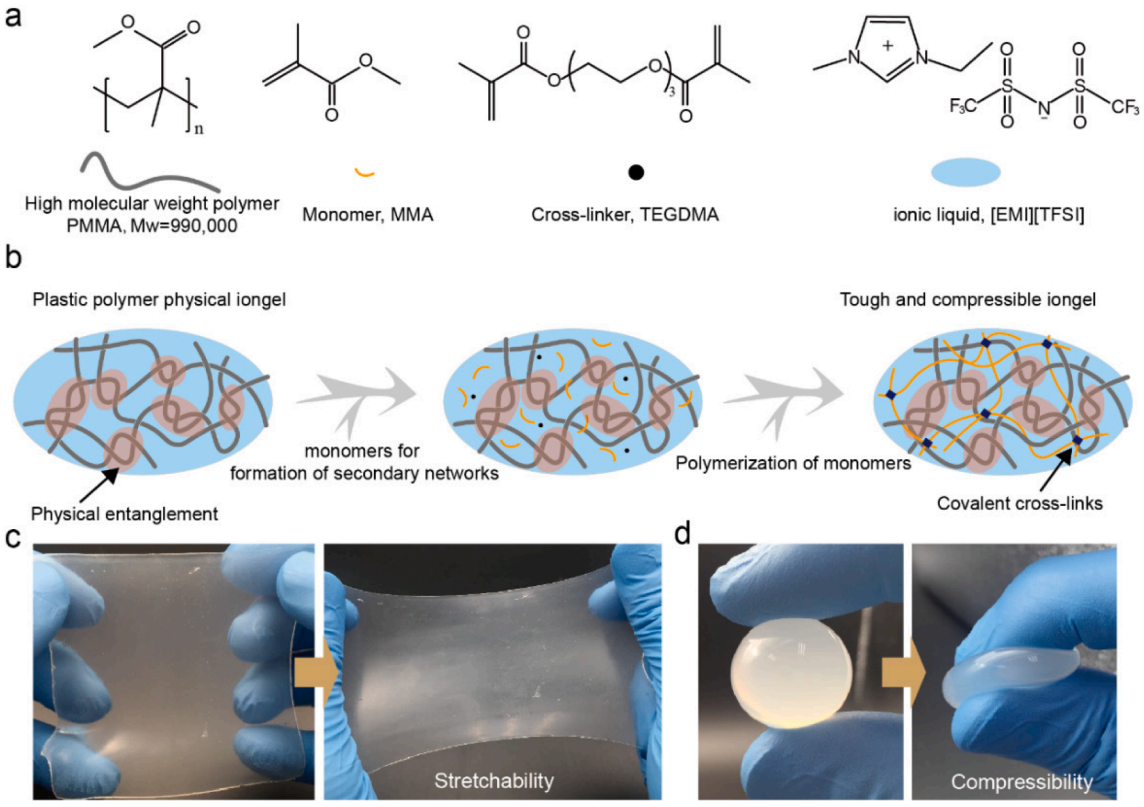


**Fig. 1.** Design of tough and compressible iongel with physically entangled network. a), Molecular structures of poly (methyl methacrylate) (PMMA), monomers, methyl methacrylate (MMA), crosslinker, triethylene glycol dimethacrylate (TEGDMA), and ionic liquid ([EMI][TFSI]). b), Schematic illustration of constructing iongel by implanting physically entangled polymer network with chemically crosslinked secondary network. Images of iongels under stretching (c) and compressing (d).

stability, reliability, and wearing comfort require sensing materials that are compressible to carry heavy loads, resilient to withstand repeated trampling underfoot, and soft to promote wearing comfort. As shown in Fig. 1a, the iongels were prepared by allowing matrix of PMMA, monomers of MMA and crosslinkers of TEGDMA to react in ionic liquid. The polymerization of monomers facilitates the formation of covalent cross-linking network structures in the iongels, resulting in good stretchability and compressibility, as presented in Fig. 1c and Fig. 1d. At the same time, we found that high molecular weight PMMA dissolved in ionic liquid would enhance the viscosity [33], and thus transform liquid iongels into plastic iongels, when PMMA content was larger than 10 % (w/w) (Fig. S1, a-c). Interestingly, liquid iongels has been demonstrated can play an important role in many applications including energy, sensing, and biomedical treatment [34–36]. More than that, physically entangled PMMA chains can interpenetrate the cross-linked network structures, formed by the polymerization of MMA monomers. As a result, the produced iongels are changed from transparent to milky white color as the increase of PMMA content (Fig. S1, d-g), owing to the increased number of physically entangled PMMA polymer chain networks. In addition, all of these iongels have good molding ability and can maintain their shape very well. These results demonstrate that the high molecular weight polymers are easy to gel and promote physical entanglement in iongels. Therefore, in our fabrication method high molecular weight PMMA (average Mw ~ 990,000 by GPC) was used to synthetize stretchable and compressible iongels.

Further investigations reveal that physical entanglement of polymer chains and high-density crosslinks play a vital role together in forming excellent elastic polymer iongels. For instance, if only containing single PMMA polymers without formation of high-density crosslinks, the obtained products were plastic polymer physical iongels. They are shear thickening, and their shape cannot be reserved (Fig. 2a and Fig. 2d). On the other hand, the cross-linked networks generated from single polymer can be regulated by changing cross-linking density [37]. When there is only MMA monomers without addition of PMMA, the products were single polymer iongels with high-density crosslinks. So, the products are very brittle and not soft due to the fracture of polymer chains (Fig. 2b and Fig. 2e). It can be concluded that there is an unavoidable choose between the softness and compression strength of iongels, and the choice achieved by adjusting the cross-linking density. When combining the plastic physically entangled chains and elastic covalently cross-

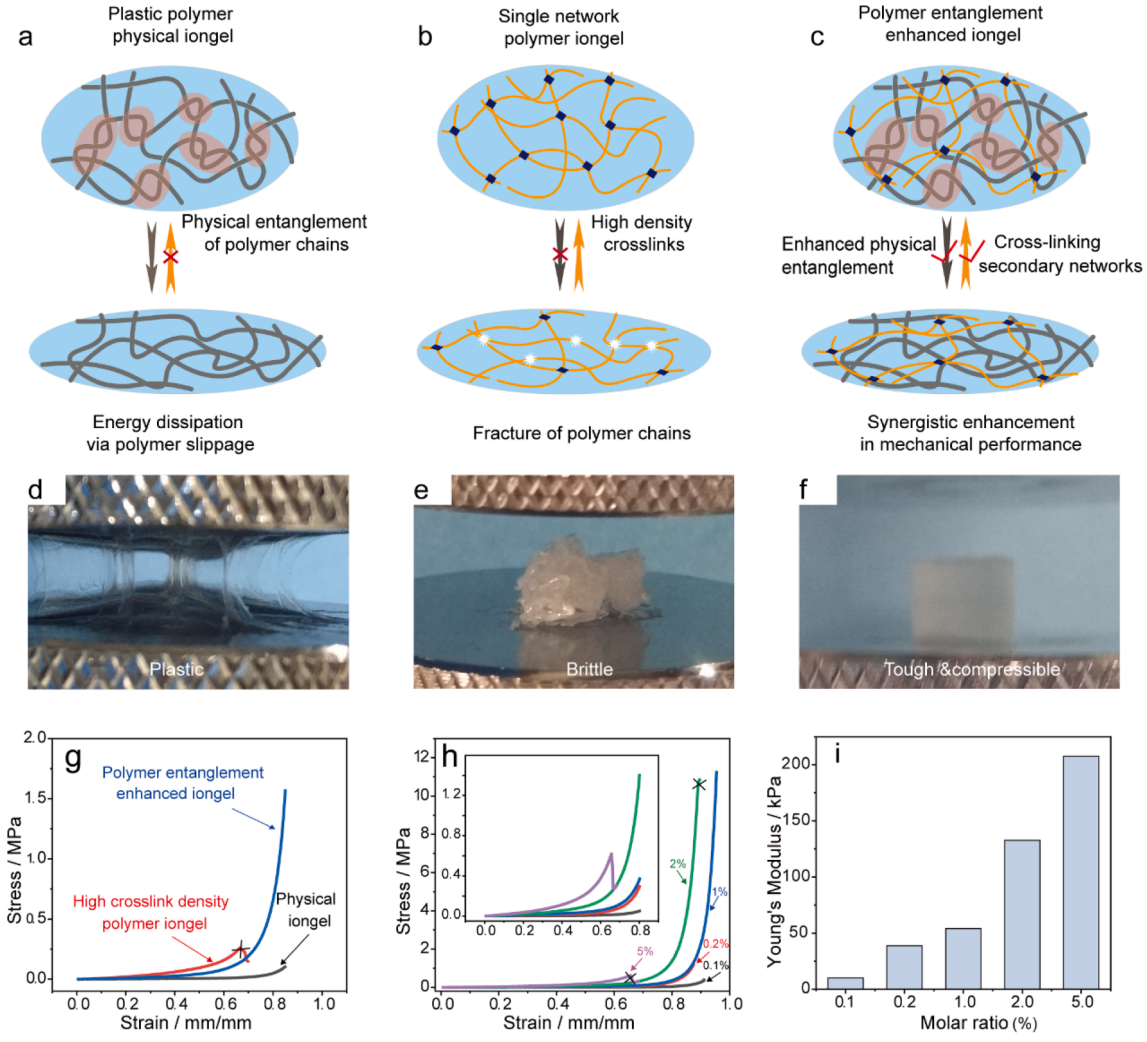


**Fig. 2.** The mechanism of mechanical enhancement of iongel by implanting physically entangled polymer network. a) Plastic polymer physical iongel that can dissipate energy via the slippages of polymer network. b) Single network polymer iongel crosslinked by chemical covalent bonds that are brittle at high crosslink density. c) Iongel with physically entangled polymer network and elastic polymer secondary network. d-f) Images of iongels after mechanical compression. g) The compression stress–strain curves of physical iongel (20 % weight percentage of PMMA in ionic liquid), high crosslink density polymer iongel (20 % weight percentage of monomer MMA with 5 % TEGDMA (TEGDMA/MMA)), and polymer entanglement enhanced iongel (20 % weight percentage of PMMA and MMA, with PMMA/MMA = 1/6, and 1 % TEGDMA). h) and i) The compression stress–strain curves of iongel with various TEGDMA content (h) and the corresponding Young's modulus of iongel (i).

linked structures to form interpenetration networks in the iongels, the high molecular weight PMMA chains tend to form densely entangled networks with crosslinks. These physically entangled and cross-linked secondary networks can dissipate energy via the reversible slippage of polymer chains. Consequently, the networks are elastic and can provide constraints in deformation to maintain resilience (Fig. 2c and Fig. 2f), and thus the as-prepared iongels are soft (low young's modulus), compressible (high compression strength), and resilient (fast recovery) (Supplementary movie-1). In a word, the designed iongels possess excellent mechanical performances and present very promising applications. These results indicate that our strategy of synthesis of stretchable and compressible iongels through enhancing physical entanglement of polymer chains and forming high-density crosslinks is successful, which can be used to fabricate other polymer materials.

### 3.2. Mechanical performance enhanced by physical entanglement

To verify the synergistic effects of physically entangled polymer chains and covalently cross-linked networks, we prepared a series of iongels with different constituents of polymer, monomer, and crosslinker to compare their mechanical performances. In the control experiments, without adding PMMA, the product was a single network iongel, which displayed a trade-off behavior between softness and compression strength due to alternation of cross-link density. Additionally, all the single network iongels were structural failures under high compression. If there is only PMMA without crosslinking, the mechanical performances of formed physical iongels are also not desired. Interestingly, when both of PMMA and monomer added, the resulting iongels are endowed with great soft, rigidity, strength as well as compressible properties together (Fig. 2g). At the same time, less crosslinker is requested to conduct the reaction. Most importantly, their mechanical strength can be controlled by changing cross-link density via alternating the content of crosslinker (TEGDMA). Their Young's modulus can be varied from ~ 10 kPa to ~ 200 kPa as the molar content of TEGDMA changed from 0.1 % to 5.0 %, respectively (Fig. 2h and Fig. 2i). These results demonstrates that covalently cross-linked secondary networks play a critical role in governing the mechanical performances of iongels. Previous studies indicate that networks comprised of permanent covalent crosslinks in the iongels are strong and durable, so they cannot be repaired or remolded and present very poor mechanical performances, owing to unable to rearrange molecules in the network [38]. Fortunately, covalently cross-linked secondary networks and other topological features, such as local fluctuations in crosslink density, can contribute to the variations of molecular force distributions. Subsequently, the mechanical properties are alternated. For example, based on a dual polymer network, iongels could be fabricated by both chemical bonding of the gelatin's amines with the polyphenol units and physical interactions between the tannic acid and the gelatin. The as-prepared iongels show flexible and elastic properties with Young's modulus between 11.3 and 28.9 kPa [39]. Besides, the combination of covalently cross-linked networks and physical interactions, can lead to remarkable stretchability and self-healing characteristics, such as the injectable iongels exhibited flexibility and high ionic conductivity [40]. In this work, covalently cross-linked secondary networks assisted by physical entanglements can form interpenetration networks in the iongels, and then dissipate energy via the reversible slippage of polymer chains. The formed network structure endows as-prepared iongels with soft, compressible, and resilient properties. These results confirm that the synergistic effects of combining physically entangled polymer chains and covalently cross-linked networks can allow the fabricated iongels to possess excellent mechanical performances.

Furthermore, we have found that the ratio of polymer (PMMA) to monomer (MMA) (P/M) also have influence on mechanical performances of iongels. As presented in Fig. 3a, their stress–strain curves are obviously different as the variation of P/M value. When the P/M value increased from 0 to 2/5, the Young's modulus is varied from ~ 35 kPa to

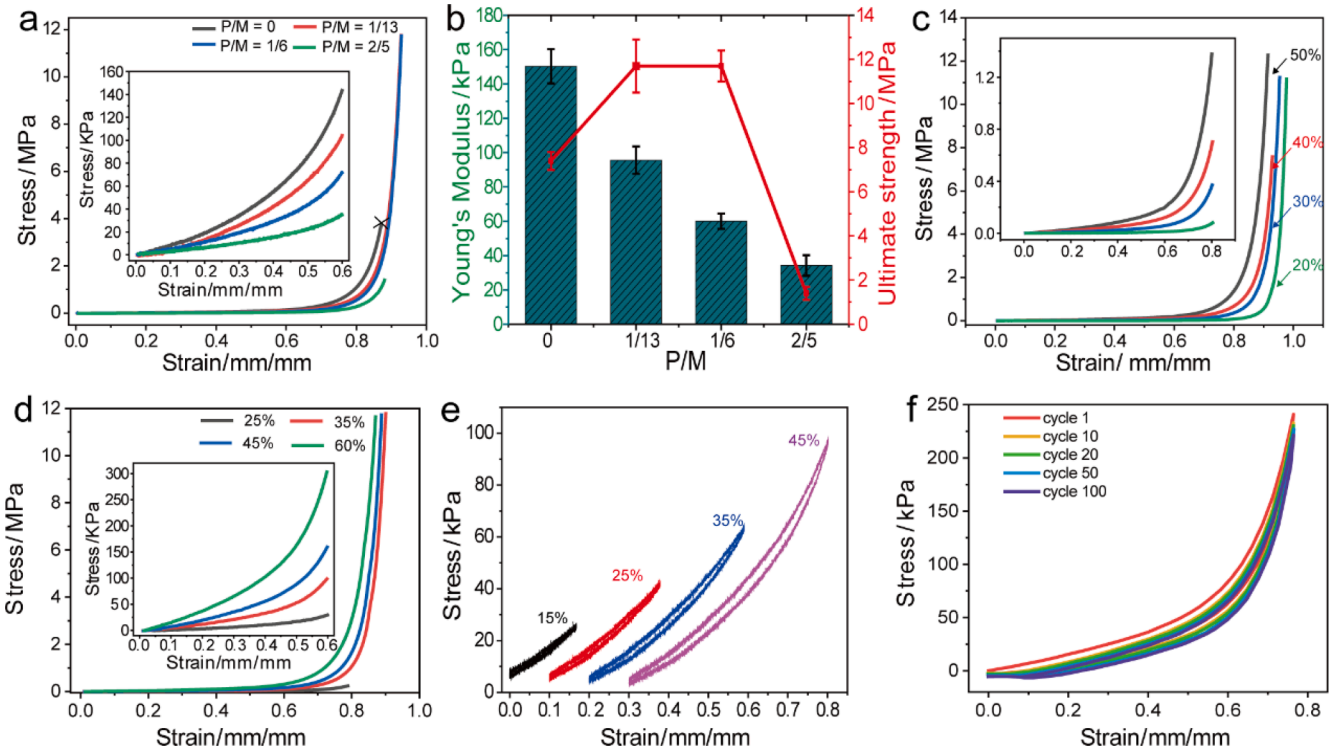


**Fig. 3.** Mechanical performance of physical entanglement enhanced iongel. a) and b) The compression stress–strain curves of iongels prepared at various ratios of polymer to monomer (P/M) under a total mass percentage of PMMA and MMA at 35 %, and the corresponding mechanical strength data. c) The compression stress–strain curves of iongels under various monomer percentages at the same content of PMMA. d) The compression stress–strain curves of iongel with various mass percentages of PMMA and MMA at P/M = 1/6. e) and f) the cyclic compression test of iongel under repeated loading–unloading cycles.

~ 150 kPa, respectively. However, the ultimate strength appeared different tendency. It has been found that the ultimate strength of iongels goes up at first and then low down as the increase of P/M value (Fig. 3b). The maximum ultimate strength is ~ 12 MPa, which is appeared during the P/M value of 1/13 and 1/6. It is because the physically entangled polymer chains will surpass the covalently crosslinked networks during high P/M value range. And the increase of viscosity will inhibit the polymerization of monomers, which leads to the formed secondary networks sparse. Thus, the resultant iongels will be very soft and dough-liked plasticity under compression (Fig. S2a). In contrast, the covalently crosslinked networks will dominate the iongel matrix during low P/M value range, and the effect of physical entanglement is not sufficient to fully dissipate energy. The two reasons cause the formed iongels to be fragile under high compression condition (Fig. S2b). When P/M value appeared at appropriate range, the resultant iongels are simultaneously endowed with excellent compressible, resilient, and soft performances (Fig. S2c).

Monomer content has been further used to optimizing the mechanical performances of iongels. Seen from the compression stress–strain curves (Fig. 3c), all prepared iongels displayed excellent mechanical performances during the variation of monomer percentages from 20 % to 50 %. It suggests there are sufficient covalently cross-linked secondary networks in the iongels under these content range of monomer. Besides, the total amount of polymers (containing PMMA and MMA) plays a key role in controlling the mechanical performances too. As shown in Fig. 3d, the total polymer content has a positive correlation with the mechanical strength of iongels. We believe that the increase of polymers amount will benefit for promoting their young's modulus and compression strength (Fig. S3). In order to investigate the resilience of iongels, the tests of loading–unloading cycles under compression strain have been conducted. It has been found that the stress–strain curves presented a narrow area under variation of compression strain, which suggests they have very good self-recover ability during compression (Fig. 3e). Their compression performances are also measured under 100 times repetitions of loading–unloading cycles at a compression strain of 75 %. And, these prepared ionogels also displayed high stability with no obvious change or weight loss after exposure in the air for several months. According to our results, these iongels present great resilience and rapid recovery ability during cyclic compression test (Fig. 3f). It demonstrates the prepared iongels possess excellent stability and reversibility. In addition, the thermogravimetric analysis (Fig. S4) suggests that there is no weight loss of iongels before 360 ℃, but PMMA would start losing weight at about 150 ℃ under the same experimental conditions. These results indicate that the as-prepared iongels possess excellent thermal stability. So, we believe that our designed iongels are extraordinary suitable for the applications of flexible wearable devices, such as plantar pressure sensor.

### 3.3. Design and performance of the plantar pressure sensor

It is well known that mechanical performances, wearing comfort and stability of the used materials is crucial for building excellent plantar pressure sensors. Especially, the designed electronic insoles for sensing should be compressible to withstand the pressure of human weight, resilient to recovery from repeated loading–unloading cycles, and wearing comfort to reduce plantar fatigue. The Young's modulus of our fabricated iongels is less than 300 kPa, which is much lower than other types of flexible conductive materials. These iongels possess advantages of excellent performances of dissipating the stress of compression through deformation in shape, very good resilience, and great recover ability from mechanical compression. At the same time, Polydimethylsiloxane (PDMS) is an elastomer material with adjustable elastic modulus and widely used in flexible devices as perfect matrix supporting materials [41]. Herein, we constructed a capacitive pressure sensor with laminated multilayer structure by using prepared iongels as flexible electrodes and PDMS silane elastomer as dielectric material and packaging layer.

Generally, sensitivity is of very importance for capacitive sensors, which can be significantly improved through designing geometric microstructures such as microtower [42], microfibers [43–45], micropyramid [46], and wrinkles [18,47]. However, the stress response range of these sensors might be narrow, as some fragile microstructures occur irreversible damage under applying large stress. For instance, the stress on the feet of an adult is about 70–150 kPa, or even much greater (more than 500 kPa) during exercise, so fragile geometric microstructures of sensors will inevitably be damaged. Therefore, the preparation of capacitive pressure sensor for real time monitoring plantar pressure not only need excellent sensitivities for detecting pressure variation but also high structural stability to bear large foot pressure. Our plantar pressure sensor was typically assembled by two parallel ionic gel electrodes sandwiching a PDMS dielectric layer (Fig. S5a-5b). The capacitance ($C$) is determined by the following equation:

$$C \propto \varepsilon \frac{A}{d}$$

where ε, d and A are the permittivity of dielectric layer, the distance between plate electrodes and the effective area of two electrodes, respectively. It can be concluded that the capacitance is varied as the change of space and area of electrode. To study the influence of capacitor structure on sensing performances, relationship between sensor sensitivity and structure parameters has been studied. The sensitivity ($S$) is defined as:

$$S = \delta(\Delta C/C_0)/\delta P$$

where $C_0$ is initial capacitance, $P$ is applied pressure, and ΔC is relative change of capacitance ($C$-$C_0$). So, the sensitivity can be obtained by calculating the slop of tangent of the curve of pressure-capacitance variation. We have investigated the influence of PDMS on the sensing performance of the capacitive pressure sensor by moderating the elastic modulus and thickness of dielectric PDMS layers (Fig. S5c-5f). The elastic modulus of PDMS can be changed by adjusting the mass ratio of the matrix and the cross-linking agent. When the mass ratio is 30:1, the elastic modulus of PDMS is similar with iongels. Both of them present good mechanical performances to perfectly match each other in flexibility. As shown in Fig. S5d, the capacitive sensors exhibit a wide response range of stress within 2 MPa, which are broad enough for realizing the real time monitoring of high foot pressure. They also present higher sensitivity in full stress range during lower modulus in dielectric layer. When the matrix ratio is 30:1 in dielectric layer, the maximum sensitivity reaches to $S > 8\ MPa^{-1}$. Significantly, when the iongels are strong enough to bear the whole-body weight, the mechanical performances of iongel electrodes display trivial effects on the sensing ability. Therefore, we employed the same constituent iongels as electrodes to construct pressure sensor in this work. In addition, the thickness of dielectric layer presented obviously negative effects on the sensitivity of sensors. So, all the dielectric layers are prepared under the matrix ratio of 20:1, due to sensors with smaller dielectric layer thickness possessing higher sensitivity (Fig. S5f).

On the other hand, the detection of high foot pressure requires a broad linear response range of a plantar pressure sensor. Hence the linear response range of sensor pressure is also very important. We find that the sensor has a good linear response even under very small stress (~kPa), which is satisfied with the monitoring of small pressure changes (Fig. 4a). Further investigations revealed that values of pressure and $\Delta C/C_0$ display the linear relationship of $Y = 0.00131X + 0.000177$ with a correlation coefficient of 0.9998. During cyclic stress tests, the stress increased from 44 kPa to 302 kPa, and the change rate of capacitance increased from 0.04 to 0.27. These results indicate that the iongel-based sensor has a very good stress variation response (Fig. 4b). Significantly, there is no obvious changes of the value of $\Delta C/C_0$ for each measurement at different loading pressures, which demonstrate that the as-prepared

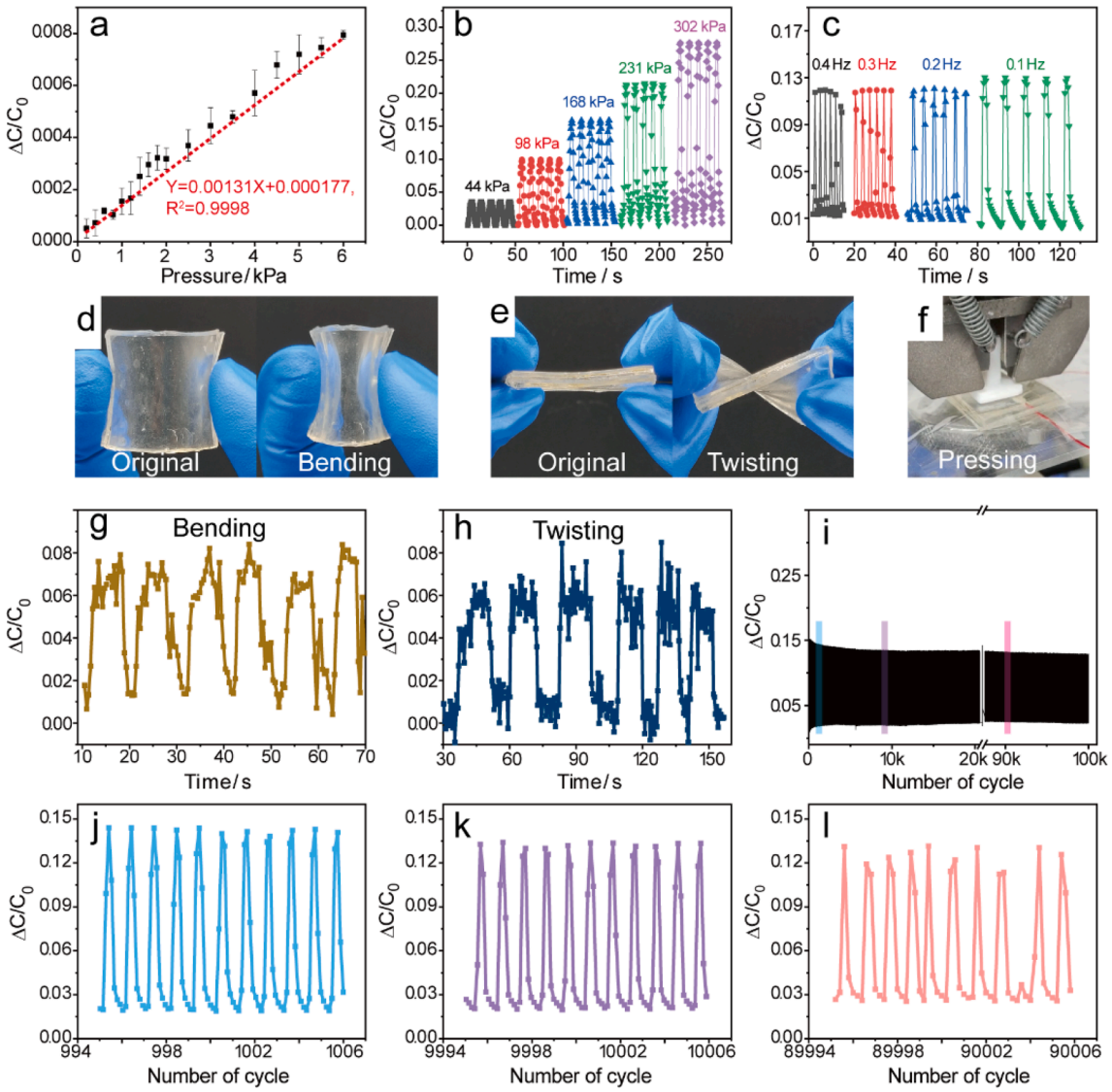


**Fig. 4.** Electric response performance of ionic gel-based pressure sensor. a) Relative capacitance variation versus pressure curve under low-pressure range (P < 6 kPa). b) Dynamic response of ionic gel-based pressure sensor to various loading pressure under a pressing frequency of 0.1 Hz. c) Dynamic response of ionic gel-based pressure sensor to various pressing frequencies under a pressure of 133 kPa. d-f) photographs of ionic gel-based pressure sensor under bending (d), twisting (e), and pressing (f). g and h) Relative capacitance variation under repeated bending (g) and twisting (h) tests. i) The durability test of ionic gel-based pressure sensor under cyclic loading–unloading pressure of 133 kPa for 100 000 cycles. j-l) Magnified capacitance response around a various number of cycles from (g).

iongel pressure sensors possess very good stability toward different weights. Considering the stress on the feet of an adult is about 70–150 kPa, we believe that our iongel pressure sensors are suitable for different weights of human and have very good stability. In addition, the capacitance-stress response at a frequency of 0.1–0.4 Hz also has been measured (Fig. 4c), which displays similar behaviors at different frequency. When the test speed alternated, the capacitance response of the sensor didn't change under the cyclic stress stimuli. So, our sensors have been demonstrated with good stability. It should be noted that our designed iongel-based capacitive sensors are capable of monitoring plantar pressure in diverse dynamic conditions (Fig. S6). Furthermore, they presented good response to bending (Fig. 4d,e) and twisting (Fig. 4g,h) measurements too, indicating high sensitivity to the detection of tiny stimulus.

To test the durability of our iongel sensor, durability measurements were also performed under a cyclic loading–unloading test with a stress of 133 kPa (Fig. 4f). In our test, the loading–unloading cycles are repeated without waiting. In contrast, the stress–strain curve of many other gels cannot fully recover even after a long waiting time [48,49]. As shown in Fig. 4i–l, the capacitance response of the sensor displays excellent stability within 100,000 cycling tests, only limited attenuation is appeared after 90,000 cycles. As we known, the durability of a pressure sensor is a key factor in long-term use reliability, especially the durability under high loading pressure. Efforts have been devoted to achieve excellent durability under high stimuli pressure in previous studies. For example, Li et al. reported that the pressure sensor can bear compression-release test over 25, 000 cycles under a high stress of 13.26 kPa [50]. In this work, our sensor demonstrates a stable cycle response of 100,000 times under a high stress of 133 kPa, showing excellent durability.

### 3.4. Sensing performance on the plantar pressure monitoring

The accurate measurement of both amplitude and spatial distribution of plantar pressure hinges on the quality of pressure sensor arrays. The size and layout of these arrays serve as crucial indicators of their spatial distribution capabilities. Particularly, for achieving precise detection of plantar pressure spatial distribution, large-area and high-

efficiency sensor arrays are indispensable. In this work, iongels are prepared by polymerizing the monomers through photo-radical polymerization reaction. Based on this special photocuring process, we used a mask patterning method to prepare the iongel sensor arrays. A 4 × 4 iongel sensor array with area of 4 × 4 $cm^2$ has been fabricated and the size of each single sensing unit is 5 × 5 $mm^2$ (Fig. 5a). The resulting sensor arrays exhibit good transparency and flexibility properties, as depicted in Fig. 5b and Fig. S7, facilitating the measurement of both spatial distribution and amplitude. As illustrated in Fig. 5c-5f, the sensor signals generated from applying different balancing weights or using various fingers are effectively differentiated quantitatively. Moreover, the entire measurement process can be completed within seconds. These findings highlight the excellent sensing capabilities of the designed iongel sensor arrays, rendering them suitable for real-time monitoring of plantar pressure. We believe that the prepared iongel sensor arrays also can be extended to design other kinds of flexible devices. For instance, synthesis of mask patterns by using photo-curing patterning method, and their size can reach to 100 μm. In a word, our prepared iongel-based sensors are suitable for designing various kinds of flexible sensing devices including mask pattern, insole, and artificial skin [51–53]. Their advantages of excellent sensing performances, good mechanical properties, large-scale preparation, and nice batch structures allow them to display very promising applications.

To realize real-time monitoring of amplitude and spatial distribution of plantar pressure, we build a plantar pressure monitoring system based on the iongel pressure sensor. As shown in Fig. 6a, the real-time plantar pressure monitoring system contains electronic insoles for pressure detection (Fig. 6a, i), analog to digital converter (Fig. 6a, ii), software of data analysis (Fig. 6a, iii), and operation interface (Fig. 6a, iv). Here, the electronic insole is a distributed 9-channel iongel pressure sensor matrix, which can real time monitor the pressure of different feet positions. The design of plantar pressure sensing system with different sensor distributions have achieved through using the convenient photo-curing patterning method of iongels. Then, we have real time monitored the plantar pressure of feet by using this system at different standing postures. The measurements of plantar pressures contain the standing postures of upright, forward and backward, respectively (Fig. 6b). The 9-channel iongel sensor has been used to realize real-time monitoring of the variations of plantar pressure of feet at different postures. When leaning forward, the value of channel 1–4 (forefoot part) increases significantly, while the value of channel 6–9 (rear heel part) decreases. In the backward condition, the value of channel 1–4 is reduced, but the value of channel 6–9 is significantly increased. Meanwhile, the channel 5 located in the arch of the foot displays little change while posture changes. The visualized sensing information of plantar pressure also commendably reflect the distribution characteristics of plantar pressure at different postures. At the same time, we studied the pressure changes of the repeated lifting and falling of the feet behaviors during simulated walking (Fig. 6c,d). During detection, the pressure of each channel can be alternately increased or decreased owing to the pressure sensor array, and the change characteristics of the plantar pressure can be real time monitored. These results demonstrate the capability of our plantar

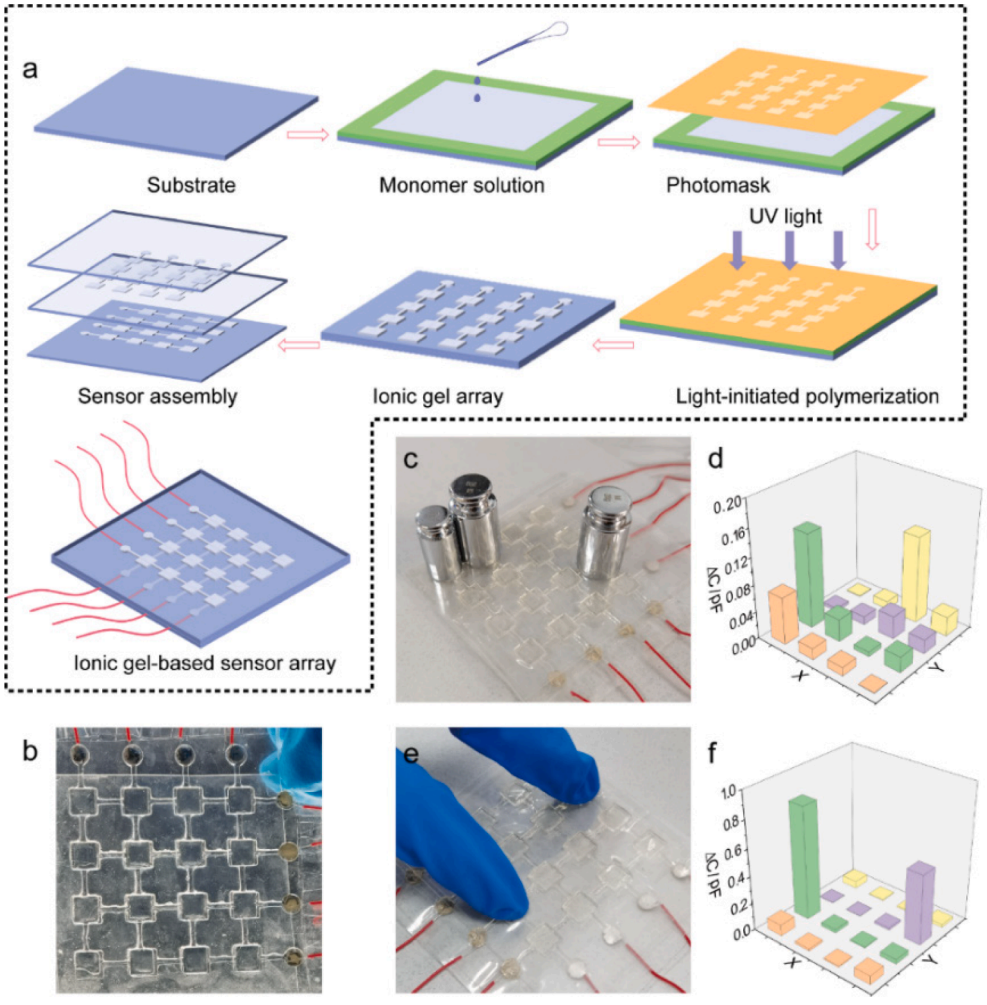


**Fig. 5.** Fabrication and performance of ionic gel-based sensor arrays. a) Schematic illustration of the fabrication of ionic gel-based sensor arrays. b) Photograph of an ionic gel-based sensor array. c-f) Sensing performance of ionic gel-based sensor arrays under weights (c and d) and finger pressing (e and f).

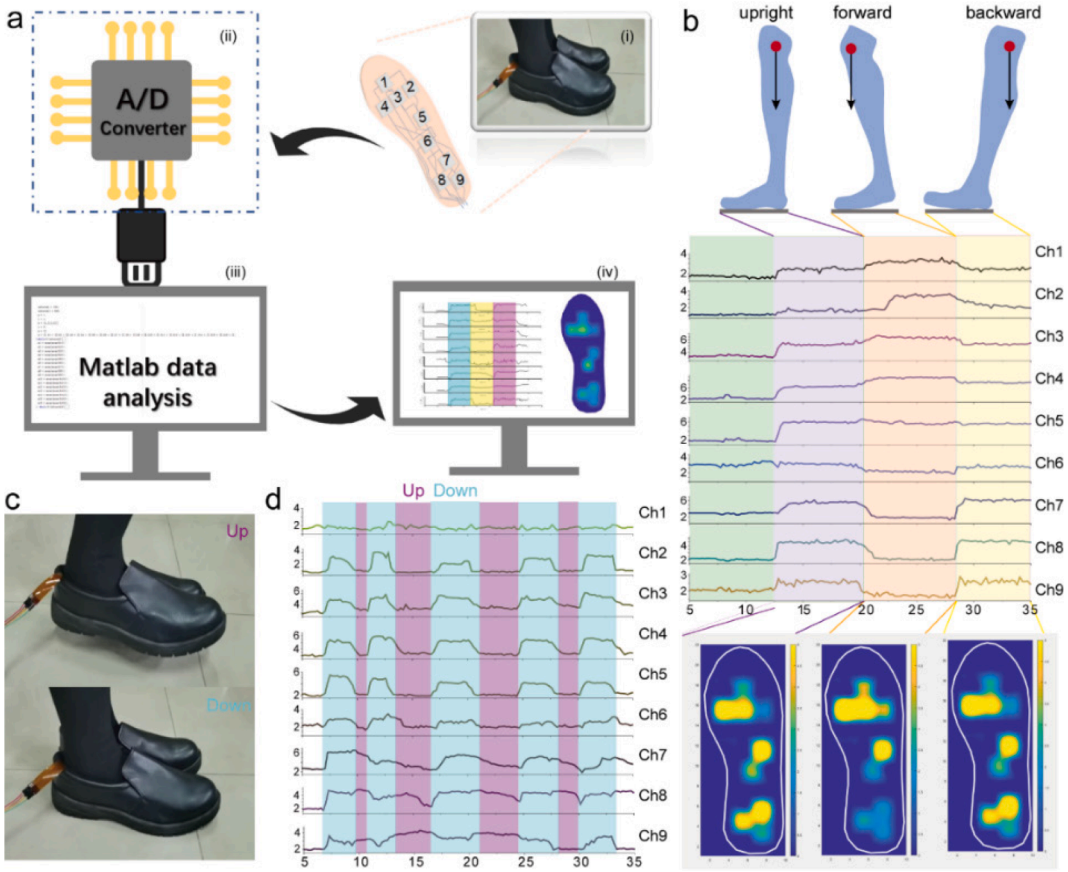


**Fig. 6.** Electronic insole based on iongel sensors and plantar pressure distribution measurement and visualization. a) Schematic illustration of plantar pressure distribution visualization system including a 9-channel pressure sensor array, analog to digital converter, data analysis software, and operation interface. b) Real-time measurement (middle) and data visualization (bottom) of plantar pressure under various standing postures (upper). Photograph (c) and real-time response of 9-channel sensor (d) under repeated foot up (purple) and down (light blue). (For interpretation of the references to color in this figure legend, the reader is referred to the web version of this article.)

pressure sensor array to track and monitor changes in plantar pressure in real-time during various static and dynamic processes. The characteristics of plantar pressure information can be digitally displayed and captured through photography for further analysis and application. For example, our plantar pressure sensor array accurately detects rapid pressure changes within seconds, as demonstrated in Fig. S8, effectively presenting real-time pressure characteristics from two different subjects. Our results indicate that the designed plantar pressure monitoring system exhibits exceptional sensitivity and boasts a rapid response to pressure fluctuations, affirming its status as an outstanding sensor system.

### *3.5. Demonstrations on sports training assistance*

Based on achievement of real-time monitoring of plantar pressure distribution by using electronic insoles and data analysis technology, we propose an intelligent application framework for plantar pressure detection (Fig. 7a). The insole is used as physical hardware for real-time monitoring of foot pressure information in body motion. Combined with simulation prediction and analysis, it can realize diversified intelligent applications of human posture analysis, fatigue prediction, rehabilitation health management, and sports training assistance. To achieve visualization of plantar pressure distribution, we use the above insoles to in situ monitor the foot pressure information in various sports involving seated row machines, treadmills, and spinning (Fig. 7, b-g). For seated rowing machine training, real-time foot pressure data reelects the distribution patterns of plantar pressure throughout various movements. During the pulling phase, the foot's interaction with the pedal significantly increases the pressure on the plantar sole, whereas this pressure diminishes upon release. Similarly, in treadmill and spinning exercises, disparities in pedal force between the front and rear soles can be accurately detected. By analyzing changes in foot pressure amplitude and positional distribution during exercise, we can predict the occurrence of exercise-induced fatigue, thereby providing timely reminders to subjects. Moreover, analysis of plantar pressure data across different sports enables us to assess athletes' sports postures, facilitating posture refinement and enhancing athletic precision.

## 4. Conclusion

The achievement of gait recognition relies on preeminent plantar pressure sensors, necessitating an ideal sensing system capable of real-time monitoring of both the magnitude and distribution of plantar pressure. Achieving such a system requires sensing materials with robust durability and reliability, especially under rigorous working conditions such as high loads, prolonged cycling, and demanding comfort requirements. In this work, we proposed a strategy to prepare PMMA conductive iongels possessing highly compliance, resilience and exceptional durability through implanting physically entangled polymer chains and covalently cross-linked networks. Our investigations reveal that the physically entangled chains enhance the compliance and the covalently crosslinked networks improve the resilience. Through fine-tuning parameters such as polymer chain length, level of physical entanglement, and density of cross-linked networks, we optimized the synergistic effects, thereby enhancing mechanical performance and expand their applications. Our results demonstrate that implanting

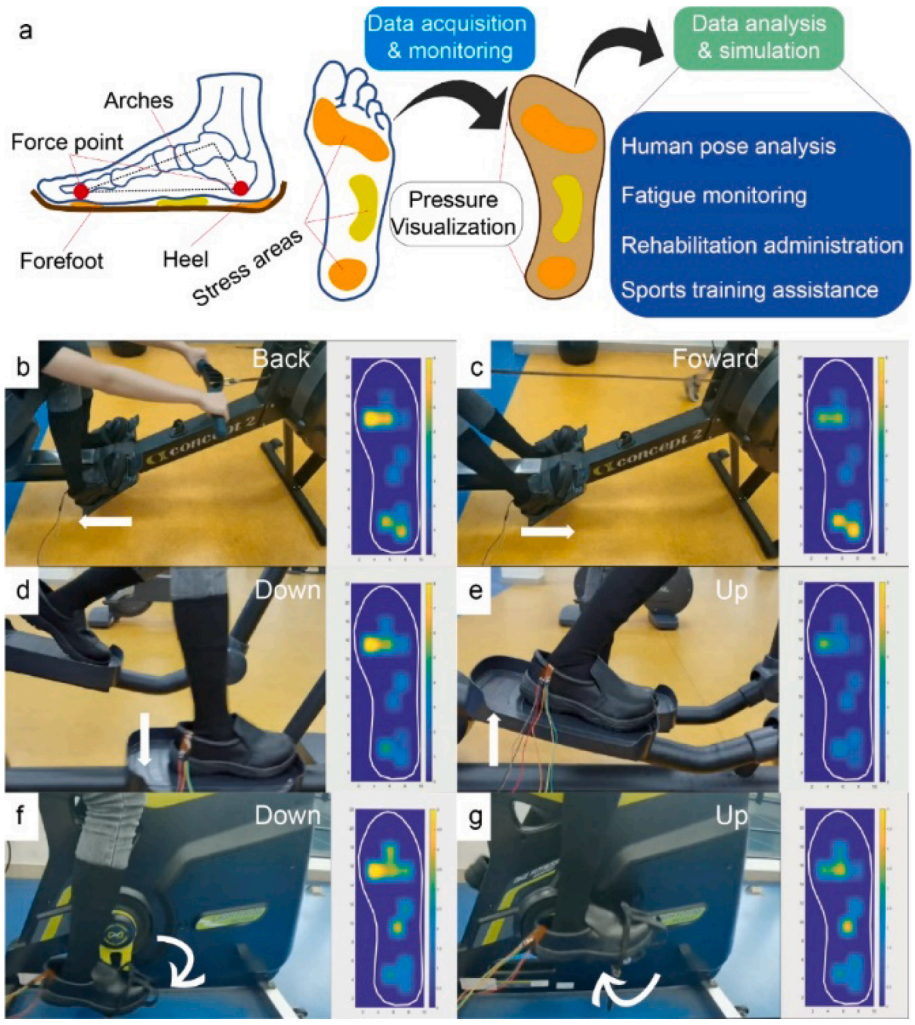


**Fig. 7.** Illustration of electronic insole for plantar pressure distribution visualization and body posture analysis. a) Proposed principal framework from plantar pressure monitor to potential applications. b-g) Plantar pressure distribution visualization for practicing seated row machine (b and c), treadmills (d and e), and spinning (f and g).

physical entanglements of polymer chains and covalently cross-linked secondary polymer networks is a powerful way for fabricating iongels with high compliance and strong resilience. Furthermore, facile operation, large scale, and high yielding make these iongels are ideal candidates for various applications.

Then, we have designed a capacitive pressure sensor utilizing the as-prepared iongels as flexible electrodes, which has exceptional long-term stability under high stress of pressure. Further studies revel that the capacitive pressure sensor has a good linear response even under very small stress (~kPa), making it suitable for monitoring subtle pressure changes in the plantar region. Significantly, the sensitivity of the capacitive pressure sensor could be controlled by moderating the elastic modulus and thickness of dielectric PDMS layer. And the thickness of dielectric layer presented obviously negative effects on sensitivity. Subsequently, the flexible electrodes were patterned into arrays via photoinitiated radical polymerization, facilitating the creation of high-precision, large-area pressure sensor arrays capable of accurately detecting spatial distribution of plantar pressure. Thereafter, we established a plantar pressure monitoring system based on the iongel pressure sensor arrays, enabling real time tracking and monitoring the changes of plantar pressure during different static and dynamic motions, including upright, forward and backward movements. The characteristics of plantar pressure information can be digitally as well as photography displayed for further analysis and applications. Moreover, the fabricated monitoring system is extremely sensitive and has a broad liner response to the pressure changes as well as very fast response speed. Considering the superior mechanical performances of our sensing materials and the simplicity of the device structure, our plantar pressure sensor offers excellent sensing performances, high durability, reliability, and wearing comfort in daily use.

In the end, the proposed intelligent application framework, combining electronic insoles with data analysis technology, successfully achieves real-time monitoring of plantar pressure, confirming their promising applications in sports training. Therefore, our researches promote fundamental understandings of simultaneously improving performances of iongel materials as well as boost the development of flexible and wearable devices. We believe that our results not only provide novel insights but also present highly promising applications across various fields including material synthesis, flexible device design, artificial skin development, and advanced sensing systems.

## CRediT authorship contribution statement

**Haifei Wang:** Writing – original draft, Methodology, Investigation, Formal analysis. **Guanhua Lin:** Writing – review & editing, Writing – original draft, Supervision, Investigation, Funding acquisition. **Yang Lin:** Methodology, Investigation. **Yang Cui:** Methodology, Investigation. **Gang Chen:** Writing – review & editing, Software. **Zhengchun**

**Peng:** Writing – review & editing, Supervision, Project administration, Funding acquisition.

## Declaration of competing interest

The authors declare that they have no known competing financial interests or personal relationships that could have appeared to influence the work reported in this paper.

## Data availability

Data will be made available on request.

## Acknowledgements

This work was supported by the joint funding program of Department of Science and Technology of Guangdong Province and the Innovation and Technology Fund of Hongkong under grant 2021A0505110015, and by the Science and Technology Innovation Council of Shenzhen under grants KQTD20170810105439418 and JCYJ20200109114237902. We also acknowledged the supporting from National Natural Science Foundation of China (21902107).

## Appendix A. Supplementary data

Supplementary data to this article can be found online at https://doi.org/10.1016/j.jcis.2024.04.137.

## References

[1] H. Seo, W.G. Chung, Y.W. Kwon, S. Kim, Y.-M. Hong, W. Park, E. Kim, J. Lee, S. Lee, M. Kim, K. Lim, I. Jeong, H. Song, J.-U. Park, Smart contact lenses as wearable ophthalmic devices for disease monitoring and health management, Chem. Rev. 123 (2023) 11488–11558.
[2] M. Bariya, H.Y.Y. Nyein, A. Javey, Wearable sweat sensors, Nat. Electron. 1 (2018) 160–171.
[3] C. Ammann-Reiffer, C.H.G. Bastiaenen, H.J.A. Van Hedel, Measuring change in gait performance of children with motor disorders: assessing the Functional Mobility Scale and the Gillette Functional Assessment Questionnaire walking scale, Dev. Med. Child Neurol. 61 (2019) 717–724.
[4] M. Chardon, F.A. Barbieri, T. Penedo, P.C.R. Santos, N. Vuillerme, The effects of experimentally-induced fatigue on gait parameters during obstacle crossing: A systematic review, Neurosci. Biobehav. Rev. 142 (2022) 104854.
[5] C. Yeh, F.-C. Kao, P.-H. Wei, A. Pal, K. Kaswan, Y.-T. Huang, P. Parashar, H.-Y. Yeh, T.-W. Wang, N. Tiwari, T.-T. Tsai, Y.-F. Huang, Z.-H. Lin, Bioinspired shark skin-based liquid metal triboelectric nanogenerator for self-powered gait analysis and long-term rehabilitation monitoring, Nano Energy 104 (2022) 107852.
[6] P. Yang, Y. Shi, S. Li, X. Tao, Z. Liu, X. Wang, Z.L. Wang, X. Chen, Monitoring the degree of comfort of shoes in-motion using triboelectric pressure sensors with an ultrawide detection range, ACS Nano 16 (2022) 4654–4665.
[7] S. Liu, J. Zhang, Y. Zhang, R. Zhu, A wearable motion capture device able to detect dynamic motion of human limbs, Nat. Commun. 11 (2020) 5615.
[8] M. Mercuri, I.R. Lorato, Y.-H. Liu, F. Wieringa, C.V. Hoof, T. Torfs, Vital-sign monitoring and spatial tracking of multiple people using a contactless radar-based sensor, Nat. Electron. 2 (2019) 252–262.
[9] J.S. Ulbrecht, T. Hurley, D.T. Mauger, P.R. Cavanagh, Prevention of recurrent foot ulcers with plantar pressure-based in-shoe orthoses: the CareFul prevention multicenter randomized controlled trial, Diabetes Care 37 (2014) 1982.
[10] J.W. Fastier-Wooller, N. Lyons, T.-H. Vu, C. Pizzolato, M. Rybachuk, T. Itoh, D. V. Dao, J. Maharaj, V.T. Dau, Flexible Iron-On Sensor Embedded in Smart Sock for Gait Event Detection, ACS Appl. Mater. Interf. 16 (2024) 1638–1649.
[11] C.B. Huang, S. Witomska, A. Aliprandi, M.A. Stoeckel, M. Bonini, A. Ciesielski, P. Samori, Molecule-graphene hybrid materials with tunable mechanoresponse: highly sensitive pressure sensors for health monitoring, Adv. Mater 31 (2019) e1804600.
[12] Y. Wan, Z. Qiu, Y. Hong, Y. Wang, J. Zhang, Q. Liu, Z. Wu, C.F. Guo, A highly sensitive flexible capacitive tactile sensor with sparse and high-aspect-ratio microstructures, Adv. Electron. Mater. 4 (2018) 1700586.
[13] X. Zhang, Z. Hu, Q. Sun, X. Liang, P. Gu, J. Huang, G. Zu, Bioinspired gradient stretchable aerogels for ultrabroad-range-response pressure-sensitive wearable electronics and high-efficient separators, Angew. Chem. Int. Ed. 62 (2023) e202213952.
[14] S. Ota, A. Ando, D. Chiba, A flexible giant magnetoresistive device for sensing strain direction, Nat. Electron. 1 (2018) 124–129.
[15] J. Tao, M. Dong, L. Li, C. Wang, J. Li, Y. Liu, R. Bao, C. Pan, Real-time pressure mapping smart insole system based on a controllable vertical pore dielectric layer, Microsyst. Nanoeng. 6 (2020) 62.
[16] C. Deng, W. Tang, L. Liu, B. Chen, M. Li, Z.L. Wang, Self-powered insole plantar pressure mapping system, Adv. Funct. Mater. 28 (2018) 1801606.
[17] Z. Wang, S. Guo, H. Li, B. Wang, Y. Sun, Z. Xu, X. Chen, K. Wu, X. Zhang, F. Xing, L. Li, W. Hu, The semiconductor/conductor interface piezoresistive effect in an organic transistor for highly sensitive pressure sensors, Adv. Mater 31 (2019) e1805630.
[18] P.Y. Chen, M. Zhang, M. Liu, I.Y. Wong, R.H. Hurt, Ultrastretchable graphene-based molecular barriers for chemical protection, detection, and actuation, ACS Nano 12 (2018) 234–244.
[19] Y. Cai, J. Shen, G. Ge, Y. Zhang, W. Jin, W. Huang, J. Shao, J. Yang, X. Dong, Stretchable $Ti_3C_2Tx$ MXene/carbon nanotube composite based strain sensor with ultrahigh sensitivity and tunable sensing range, ACS Nano 12 (2018) 56–62.
[20] B.W. An, S. Heo, S. Ji, F. Bien, J.U. Park, Transparent and flexible fingerprint sensor array with multiplexed detection of tactile pressure and skin temperature, Nat. Commun. 9 (2018) 2458.
[21] M. Lin, Z. Zheng, L. Yang, M. Luo, L. Fu, B. Lin, C. Xu, A. High-Performance, Sensitive, wearable multifunctional sensor based on Rubber/CNT for human motion and skin temperature detection, Adv. Mater. 34 (2021) 2107309.
[22] C. García Núñez, L. Manjakkal, R. Dahiya, Energy autonomous electronic skin, npj Flex Electron. 3 (2019) 1.
[23] C. Yang, Z. Suo, Hydrogel ionotronics, Nat. Rev. Mater. 3 (2018) 125–142.
[24] H. Yuk, J. Wu, X. Zhao, Hydrogel interfaces for merging humans and machines, Nat. Rev. Mater. 7 (2022) 935–952.
[25] G. Chen, X. Xiao, X. Zhao, T. Tat, M. Bick, J. Chen, Electronic textiles for wearable point-of-care systems, Chem. Rev. 122 (2022) 3259–3291.
[26] M. Hua, S. Wu, Y. Ma, Y. Zhao, Z. Chen, I. Frenkel, J. Strzalka, H. Zhou, X. Zhu, X. He, Strong tough hydrogels via the synergy of freeze-casting and salting out, Nature 590 (2021) 594.
[27] S. Lin, J. Liu, X. Liu, X. Zhao, Muscle-like fatigue-resistant hydrogels by mechanical training, Proc. Natl. Acade. Sci. USA 116 (2019) 10244–10249.
[28] X. Le, W. Lu, J. Zhang, T. Chen, Recent progress in biomimetic anisotropic hydrogel actuators, Adv. Sci. 6 (2019) 1801584.
[29] J. Kim, G. Zhang, M. Shi, Z. Suo, Fracture, fatigue, and friction of polymers in which entanglements greatly outnumber cross-links, Science 374 (2021) 212–216.
[30] I. del Agua, D. Mantione, N. Casado, A. Sanchez-Sanchez, G.G. Malliaras, D. Mecerreyes, Conducting polymer iongels based on PEDOT and guar gum, ACS Macro Lett. 6 (2017) 473–478.
[31] Z. Li, S. Chang, S. Khuje, S. Ren, Recent advancement of emerging nano copper-based printable flexible hybrid electronics, ACS Nano 15 (2021) 6211–6232.
[32] C. Liu, N. Morimoto, L. Jiang, S. Kawahara, T. Noritomi, H. Yokoyama, K. Mayumi, K. Ito, Tough hydrogels with rapid self-reinforcement, Science 372 (2021) 1078–1081.
[33] M.P. Scott, C.S. Brazel, M.G. Benton, J.W. Mays, J.D. Holbrey, R.D. Rogers, Application of ionic liquids as plasticizers for poly(methyl methacrylate), Chem. Commun. 1370–1371 (2002).
[34] Y. Gao, W. Zhang, L. Li, Z. Wang, Y. Shu, J. Wang, Ionic liquid-based gels for biomedical applications, Chem. Eng. J. 452 (2023) 139248.
[35] F. Ghorbanizamani, H. Moulahoum, E. Guler Celik, S. Timur, Ionic liquids enhancement of hydrogels and impact on biosensing applications, J. Molecul. Liquid. 357 (2022) 119075.
[36] D. Valverde, A. Garcia-Bernabé, A. Andrio, E. García-Verdugo, S.V. Luis, V. Compañ, Free ion diffusivity and charge concentration on cross-linked polymeric ionic liquid iongel films based on sulfonated zwitterionic salts and lithium ions, Phys. Chem. Chem. Phys. 21 (2019) 17923–17932.
[37] M.A. Susan, T. Kaneko, A. Noda, M. Watanabe, Ion gels prepared by in situ radical polymerization of vinyl monomers in an ionic liquid and their characterization as polymer electrolytes, J. Am. Chem. Soc. 127 (2005) 4976–4983.
[38] S.P.O. Danielsen, H.K. Beech, S. Wang, B.M. El-Zaatari, X. Wang, L. Sapir, T. Ouchi, Z. Wang, P.N. Johnson, Y. Hu, D.J. Lundberg, G. Stoychev, S.L. Craig, J.A. Johnson, J.A. Kalow, B.D. Olsen, M. Rubinstein, Molecular characterization of polymer networks, Chem. Rev. 121 (2021) 5042–5092.
[39] A. Aguzin, G.C. Luque, L.I. Ronco, I. del Agua, G. Guzmán-González, B. Marchiori, A. Gugliotta, L.C. Tomé, L.M. Gugliotta, D. Mecerreyes, R.J. Minari, Gelatin and tannic acid based iongels for muscle activity recording and stimulation electrodes, ACS Biomater. Sci. Eng. 8 (2022) 2598–2609.
[40] V. Zhang, B. Kang, J.V. Accardo, J.A. Kalow, Structure–reactivity–property relationships in covalent adaptable networks, J. Am. Chem. Soc. 144 (2022) 22358–22377.
[41] W. Dong, R. Zhang, G. Lin, Molecular-level design of excellent reversible thermochromic polydiacetylene materials with the simultaneous enhancement of multiple performances, Mater. Chem. Front. 5 (2021) 7041–7050.
[42] C.M. Boutry, A. Nguyen, Q.O. Lawal, A. Chortos, S. Rondeau-Gagne, Z. Bao, A sensitive and biodegradable pressure sensor array for cardiovascular monitoring, Adv. Mater 27 (2015) 6954–6961.
[43] Y. Bin Shin, C. Jong Han, Y. Kim, J.-W. Kim, Ultrareproducible Capacitive Soft Pressure Sensor Using a Self-Integrated Fibrous Network of Urethane Equipped with Diels-Alder Adducts, Adv. Eng. Mater. 24 (2022) 2100903.
[44] C.B. Cooper, K. Arutselvan, Y. Liu, D. Armstrong, Y. Lin, M.R. Khan, J. Genzer, M. D. Dickey, Stretchable capacitive sensors of torsion, strain, and touch using double helix liquid metal fibers, Adv. Funct. Mater. 27 (2017) 1605630.
[45] C. Wang, K. Xia, M. Jian, H. Wang, M. Zhang, Y. Zhang, Carbonized silk georgette as an ultrasensitive wearable strain sensor for full-range human activity monitoring, J. Mater. Chem. C 5 (2017) 7604–7611.
[46] C. Wu, T. Zhang, J. Zhang, J. Huang, X. Tang, T. Zhou, Y. Rong, Y. Huang, S. Shi, D. Zeng, A new approach for an ultrasensitive tactile sensor covering an ultrawide

pressure range based on the hierarchical pressure-peak effect, Nanoscale Horiz. 5 (2020) 541–552.
[47] X. Tang, C. Wu, L. Gan, T. Zhang, T. Zhou, J. Huang, H. Wang, C. Xie, D. Zeng, Multilevel microstructured flexible pressure sensors with ultrahigh sensitivity and ultrawide pressure range for versatile electronic skins, Small 15 (2019) 1804559.
[48] Q. Zhang, X. Liu, L. Duan, G. Gao, Nucleotide-driven skin-attachable hydrogels toward visual human–machine interfaces, J. Mater. Chem. A 8 (2020) 4515–4523.
[49] J.-Y. Sun, X. Zhao, W.R.K. Illeperuma, O. Chaudhuri, K.H. Oh, D.J. Mooney, J. J. Vlassak, Z. Suo, Highly stretchable and tough hydrogels, Nature 489 (2012) 133–136.
[50] Y. Cheng, Y. Xie, Z. Liu, S. Yan, Y. Ma, Y. Yue, J. Wang, Y. Gao, L. Li, Maximizing electron channels enabled by MXene aerogel for high-performance self-healable flexible electronic skin, ACS Nano 17 (2023) 1393–1402.
[51] S. Zhang, L. Lu, S. Wang, F. Yuan, S. Xuan, X. Gong, Coaxial direct ink writing of shear stiffening gel/Ecoflex composite for customized insoles, Compos. Part B-Eng. 225 (2021) 109268.
[52] J.-H. Choi, Y. Gu, K. Hong, W. Xie, C.D. Frisbie, T.P. Lodge, High capacitance, photo-patternable ion gel gate insulators compatible with vapor deposition of metal gate electrodes, ACS Appl. Mater. Interf. 6 (2014) 19275–19281.
[53] M. Amjadi, K.-U. Kyung, I. Park, M. Sitti, Stretchable, skin-mountable, and wearable strain sensors and their potential applications: a review, Adv. Funct. Mater. 26 (2016) 1678–1698.